

Statistical analysis of electronic properties of alkanethiols in metal–molecule–metal junctions

Tae-Wook Kim¹, Gunuk Wang¹, Hyoyoung Lee² and Takhee Lee¹

¹ Heeger Center for Advanced Materials and Department of Materials Science and Engineering, Gwangju Institute of Science and Technology, Gwangju 500-712, Korea

² National Creative Research Initiatives, Center for Smart Molecular Memory, IT Convergence Components Laboratory, Electronics and Telecommunication Research Institute, Daejeon 305-350, Korea

E-mail: tlee@gist.ac.kr

Received 2 March 2007, in final form 29 April 2007

Published 6 July 2007

Online at stacks.iop.org/Nano/18/315204

Abstract

We fabricated 13 440 molecular electronic devices using different lengths of alkanethiol self-assembled monolayers and performed statistical analyses on the histograms of the electronic transport properties of the alkanethiols. The statistical analysis provides criteria for defining ‘working’ molecular electronic devices and selecting ‘representative’ devices. The yield of the working alkanethiol devices was found to be ~1.2% (156 out of 13 440 devices) and average transport parameters such as current density, transport barrier height, effective electron mass and tunnelling decay coefficient were obtained from the statistically defined working molecular electronic devices. From the length-dependent tunnelling and temperature-variable current–voltage characteristics of the working devices, the alkanethiol molecular devices showed typical tunnelling transport. However, the statistical consideration for determining working molecular devices should be carried out prior to these characterizations or detailed analysis on them.

(Some figures in this article are in colour only in the electronic version)

1. Introduction

Due to the merits such as low cost, high density and less heat problems for using functional molecules as nanoscale building blocks in miniaturized electronic devices, molecular electronics is currently undergoing rapid development, although poor reproducibility and low device yield still remains a challenge [1–6]. Extensive efforts have been made to understand charge transport in molecular layers [7, 8]. Alkanethiol ($\text{CH}_3(\text{CH}_2)_{n-1}\text{SH}$) self-assembled monolayers (SAMs) on Au surfaces are one of the most extensively studied molecular systems because of the robust formation of monolayers of alkanethiols on a Au surface [3, 9]. The yield of molecular electronic devices of even these robust alkanethiol molecular systems, however, is very low, mainly because of electrical shorts caused by the penetration of the top electrode through the molecular layer and making contact with the bottom electrode [10, 11]. A recent study, with the objective

of preventing electrical shorts by using a layer of a highly conducting polymer, resulted in a significant improvement in the yield of molecular electronic devices [7]. However, studies on the device yield of simple metal–molecule–metal (M–M–M) junctions have not been extensive. In particular, systematic studies with the goal of defining ‘working’ molecular devices, device yield and even selecting ‘representative’ devices have not been reported. Furthermore, determining the average transport parameters from a statistically meaningful number of molecular working devices is important because the statistically averaged transport parameters can provide more accurate and meaningful characteristics of molecular systems. Statistical measurements have been performed, for example, to extract the electrical conductance of single molecules using mechanically controllable break junctions [12].

In this study, we fabricated a large number of alkanethiol molecular electronic devices (13 440) as vertical M–M–M

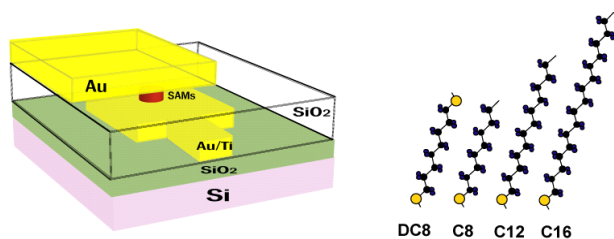


Figure 1. A schematic diagram of a metal–alkanethiol–metal junction device and molecular structures of octanedithiol (DC8), octanethiol (C8), dodecanethiol (C12) and hexadecanethiol (C16).

structures, without using any intermediate external polymer layer which might cause an additional interface to be produced in the molecular junctions, and characterized their electronic transport properties. Gaussian distribution functions were used to statistically analyse the mass-fabricated molecular devices and a simple criterion for the statistical determination of working devices and representative devices is proposed. Average transport parameters such as current density, transport barrier height, effective electron mass and tunnelling decay coefficient were obtained from the statistically defined working molecular electronic devices. In addition, the statistical criterion was employed to demonstrate that determining working molecular electronic devices should be done prior to further analysis such as temperature-variable characterization on the devices. Also, the statistical analysis would be useful for comparing the transport parameters of different molecular systems.

2. Experimental details

The alkanethiol M–M–M junction devices were fabricated on a p-type (100) Si substrate covered with a thermally grown 3000 Å thick layer of SiO₂. As schematically illustrated in figure 1, the conventional optical lithography method was used to pattern bottom electrodes that were prepared with Au (1000 Å)/Ti (50 Å) using an electron beam evaporator. A SiO₂ layer (700 Å thick) was deposited on the patterned bottom electrodes by plasma-enhanced chemical vapour deposition (PECVD). Reactive ion etching (RIE) was then performed to produce microscale via-holes of 2 μm diameter through the SiO₂ layer to expose the Au surfaces of the bottom electrodes. Four different ~5 mM alkanethiol solutions were prepared by adding ~10 μl alkanethiols to ~10 ml anhydrous ethanol (from Aldrich Chem. Co.). The chips were left in the solution for 24–48 h for the alkanethiol self-assembled monolayers (SAMs) to assemble on the Au surfaces exposed by RIE in a nitrogen-filled glove box with an oxygen level of less than ~10 ppm. Alkanethiols (from Aldrich Chem. Co.) of different structures and lengths: octanedithiol (HS(CH₂)₈SH, denoted as DC8), octanethiol (CH₃(CH₂)₇SH, C8), dodecanethiol (CH₃(CH₂)₁₁SH, C12), and hexadecanethiol (CH₃(CH₂)₁₅SH, C16), were used to form the active molecular components. After the alkanethiol SAMs were formed on the exposed Au surfaces, a top Au electrode was produced by thermal evaporation to form M–M–M junctions. This evaporation was done with a shadow mask on the chips with a liquid nitrogen cooled cold stage in order to minimize thermal damage to the

active molecular component under a pressure of ~10⁻⁶ Torr. For the same reason, the deposition rate for the top Au electrode was kept very low, typically ~0.1 Å s⁻¹ until the total thickness of the top Au electrode reached ~500 Å. Figure 1 shows a schematic diagram of a microscale M–M–M junction device and molecular structures of different alkanethiols. The room temperature current–voltage (*I*–*V*) characteristics of the fabricated molecular devices were evaluated using a HP4155A semiconductor parameter analyser. The fabricated chips were packaged and loaded into a cryostat (from Janis Co.). The temperature was varied from 300 to 77 K by flowing liquid nitrogen into the sample holder in the vacuum chamber.

3. Results and discussion

As mentioned above, the yields of the molecular electronic devices are very low, mainly due to electrical shorting problems [10, 11, 13]. However, thorough and systematic studies on what ‘working’ devices are and on the yields of the molecular electronic devices have not been reported. Typically, a working device might be defined as a device showing nonlinear *I*–*V* behaviour and not being electrical open and short. Electrical open and short devices can be readily recognized. Open devices are noisy with a current level typically in the picoampere range and short devices show ohmic *I*–*V* characteristics with a current level larger than a few milliamperes [14]. However, criteria are needed for determining working devices more precisely. Although the choice of such a criterion is not universal, current density can be a good criterion for determining working devices, because *I*–*V* data are major characteristics that are measured initially and the current directly reflects the conductivity of different lengths of alkanethiols or different molecular systems.

For this study, we fabricated a statistically sufficient number of molecular devices and characterized their electronic properties to obtain reasonable criteria for defining working devices and device yield. Specifically, we fabricated 13 440 molecular electronic devices of alkanethiol SAMs (C8, C12 and C16 SAMs) with a microscale via-hole structure, as shown in figure 1. We then statistically analysed all of the fabricated devices. From the *I*–*V* characterizations of all 13 440 devices, 11 744 showed electrical shorts. The devices with an electrical short showed short-circuit ohmic *I*–*V* characteristics and a current typically larger than 10 mA at 1.0 V. Fabrication failure (392) and electrical open devices (1103) occurred mainly because of failures during the fabrication process. The electrical open devices show noisy and open circuit *I*–*V* behaviours. We then performed a statistical analysis on the remaining 201 ‘candidate’ working devices as follows. First, we plotted histograms of the logarithmic current densities ($\log J$) of the C8, C12 and C16 candidate working devices and then performed Gaussian fittings on the histograms using the normal distribution function,

$$f(x) = \frac{1}{\sigma\sqrt{2\pi}} \exp\left[-\frac{(x-\mu)^2}{2\sigma^2}\right] \quad (1)$$

where μ is the average and σ is the standard deviation. We selected the 99.7% of the devices from the overall population which are included in the interval of the 3σ range between

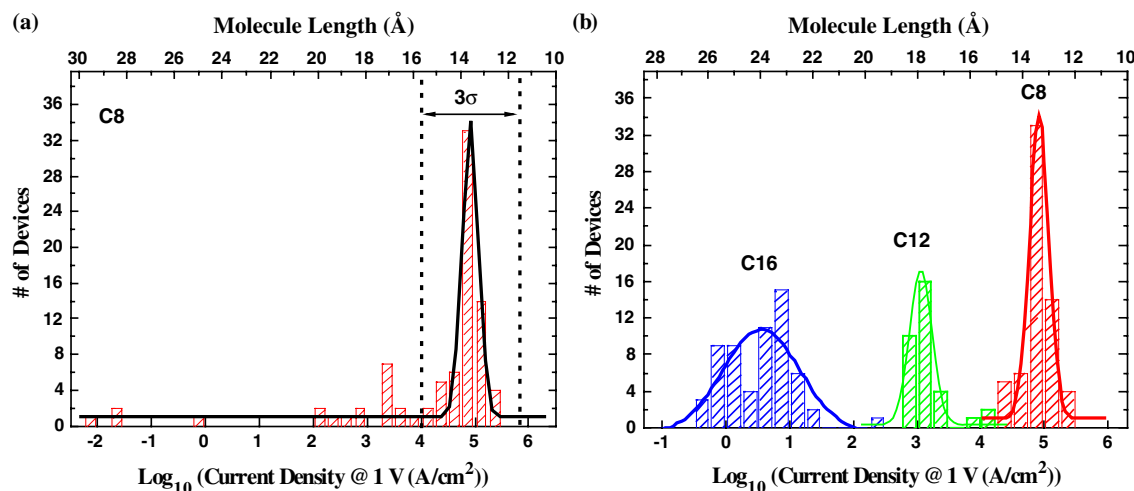


Figure 2. (a) Histogram of logarithmic current densities at 1 V for ‘candidate’ C8 molecular electronic devices. (b) Histograms of current densities at 1 V for ‘working’ C8, C12 and C16 devices. (See text for the definition of candidate and working devices.) Solid lines are Gaussian fitting curves.

Table 1. Summary of results for the fabricated devices. (Note: working and non-working devices were defined by statistical analysis with Gaussian fitting on histograms of the logarithmic scale current densities (see text).)

	# of fabricated devices	Fab. failure	Short	Open	Non-working	Working				Device yield
						DC8	C8	C12	C16	
Monothiol	13 440 (100%)	392 (2.9%)	11 744 (87.4%)	1103 (8.2%)	45 (0.3%)	63 (1.41%)	33 (0.69%)	60 (1.44%)	156 (1.2%)	
Dithiol	4800 (100%)	192 (4%)	4080 (85%)	428 (8.9%)	16 (0.3%)	84 (1.75%)			84 (1.75%)	

$\mu + 3\sigma$ and $\mu - 3\sigma$. This 3σ range was chosen arbitrarily to include as many devices as possible. When current densities are within the 3σ range (indicated as dotted lines in figure 2(a)), they are defined as working molecular electronic devices whereas the others are defined as ‘non-working’ devices when the current densities are outside this range. Figure 2(a) shows an example of a histogram plot for logarithmic current densities of all C8 candidate devices. One can see that some of the non-working devices are located outside the 3σ range. Similarly, we are able to define the working device ranges of C12 and C16 devices. Figure 2(b) shows a summarized histogram plot of the current densities at 1 V for all of the working C8, C12 and C16 devices, based on the statistical analysis. This graph shows the difference in current density levels for different lengths of alkanethiols. Here, we consider that the electronic conduction is mainly so-called ‘through-bond’ tunnelling, that is, electrons flow along the all-trans alkyl chain via the overlapping σ -bonds. Therefore, the tunnelling rate is independent of the molecular-chain tilt with respect to the substrate. Instead, it depends only on the molecular length [15, 16]. In spite of a slight overlap around the tails of the intervals of three different alkanethiols in figure 2(b), each alkanethiol shows a unique current density range. By using the relationship $\ln(J) \propto -\beta d$ which means the known exponential dependence of tunnelling current through alkanethiols [11, 13, 18–21] and assigning the known molecular lengths for C8 (13.3 Å) and C16 (23.2 Å) at the mean current densities of C8 and C16 devices [11],

we deduced the relationship between the logarithmic current at the entire bottom axis and the molecular length at the top axis, shown in figure 2(b). Then, the molecular length at the mean current density of C12 devices was determined as 18.2 Å from figure 2(b), the known molecular length of C12 [11]. Thus, figure 2 shows that the logarithmic current density is linearly dependent on molecular length, suggesting the exponential length-dependent charge transport through the alkanethiols [11, 13, 18–21]. Therefore, the current density is significantly affected by a slight change in molecular length. One can note that the histograms in figure 2 show the distribution of the logarithmic current densities, indicating the existence of a fluctuation factor causing the exponential distribution in the current densities. This fluctuation factor could be the tunnelling distance, indicating that fluctuations in molecular configurations in the self-assembled monolayers in the device junctions are possible, such as molecular tilting angle and surface flatness of the Au bottom electrode on which the molecules are assembled [17].

The values of $\{\mu, \sigma\}$ for the logarithmic current densities at 1 V for C8, C12 and C16 were found to be {4.87, 0.23}, {3.15, 0.29} and {0.533, 0.527}, respectively. Among the above-mentioned 201 candidate devices, 45 were found to be non-working devices and 156 were determined to be working devices, using the statistical criteria (3σ range). As summarized in table 1, the numbers of C8, C12 and C16 working devices were 63, 33 and 60, respectively, among the total 13 440 fabricated devices. Thus, the device yield

is $\sim 1.2\%$ (156/13440). This device yield $\sim 1.2\%$ was determined using the 3σ range criterion. If more narrow ranges such as the 2σ range or the 1σ range are used, the device yield is reduced to $\sim 1.1\%$ (142/13440) or $\sim 1.0\%$ (132/13440), respectively. The similar statistical analysis was also performed for the octanedithiol (DC8) molecule to demonstrate the device yield for different molecular devices. In this case dithiol has both chemisorbed contacts [Au–S] at both sides to metal electrodes whereas monothiol has one chemisorbed contact and the other physisorbed contact [Au–CH₃]. As shown in table 1, the device yield ($\sim 1.75\%$) of DC8 dithiol devices is not so much different from that of C8 monothiol devices. This result may suggest that device yield is not much affected by the metal–molecular contact, but rather affected more by the device structures, fabrication condition, and quality of the self-assembled monolayer.

As mentioned above, the main reason for such a very low device yield is because the top Au contacts penetrate the thin molecular monolayer and make contact with the bottom electrode [10, 11, 13]. It should be noted that the device yield of $\sim 1.2\%$ applies to the vertical structures of microscale molecular electronic devices, and may not be the same for the vertical structures of nanoscale devices [18, 22] or horizontal structures such as break junction [23] and electromigration nanogap devices [24].

A number of groups have demonstrated that the charge transport through alkanethiol SAMs is tunnelling and can be explained by the Simmons tunnelling model [18, 25–27] as

$$J = \left(\frac{e}{4\pi^2 \hbar d^2} \right) \left\{ \left(\Phi_B - \frac{eV}{2} \right) \exp \left[-\frac{2(2m)^{1/2}}{\hbar} \times \alpha \left(\Phi_B - \frac{eV}{2} \right)^{1/2} d \right] - \left(\Phi_B + \frac{eV}{2} \right) \times \exp \left[-\frac{2(2m)^{1/2}}{\hbar} \alpha \left(\Phi_B + \frac{eV}{2} \right)^{1/2} d \right] \right\} \quad (2)$$

where m is the electron mass, d is the barrier width, Φ_B is the barrier height, V is the applied bias and α is a unitless adjustable parameter that can be used to differentiate between potential barrier shapes, or to describe the effective mass of the electron. This Simmons tunnelling fitting was done on all the working C8, C12 and C16 devices (total 156 devices) to obtain the statistical Φ_B and α values. The molecular lengths used in this work are 13.3, 18.2 and 23.2 Å for C8, C12 and C16, respectively, determined by adding an Au–thiol bond length to the length of the original molecule [28]. Figures 3(a) and (b) show the distribution for the Simmons fitting results, Φ_B and α values of all of the individual working C8, C12 and C16 devices. The current densities for the different length alkanethiols exhibit exponential length-dependent transport, characterized by a tunnelling decay coefficient β [1, 13, 18–21]. The β value in the low bias range can be defined from the Simmons equation (equation (2)) as follows:

$$\beta = \frac{2(2m)^{1/2}}{\hbar} \alpha (\Phi_B)^{1/2}. \quad (3)$$

The β values were calculated for all of the individual working devices and are summarized in figure 3(c).

The Φ_B (figure 3(a)) and α (figure 3(b)) values obtained from Simmons fitting increase and decrease with

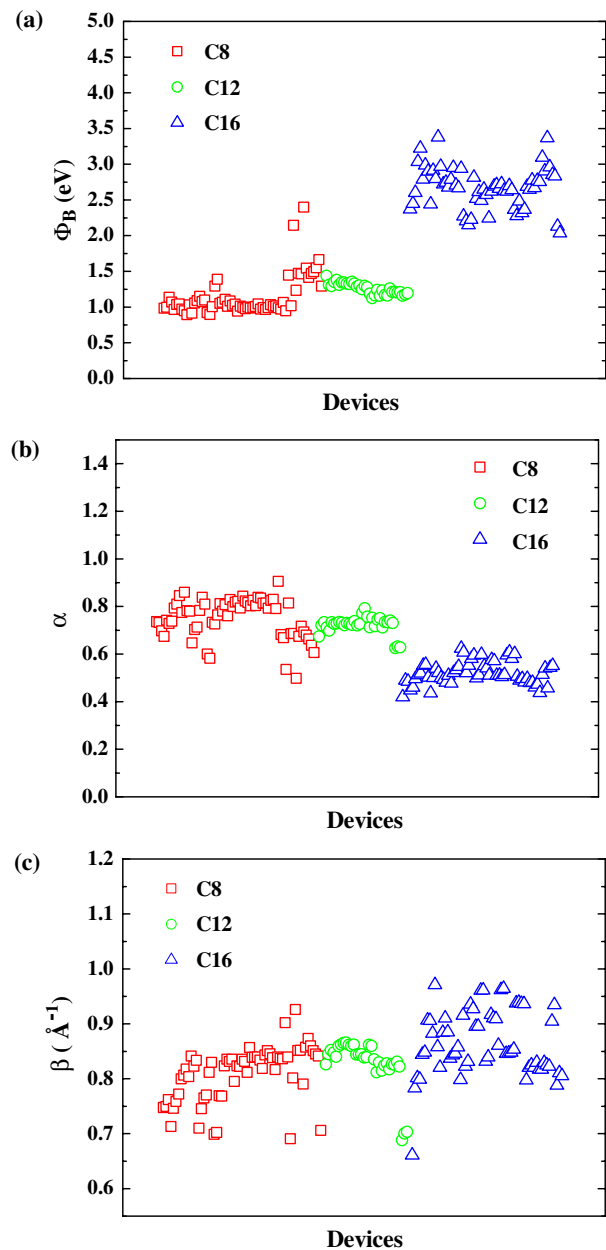


Figure 3. Distribution in transport barrier height Φ_B (a), parameter α (b) and decay coefficient β (c) for all of the working C8, C12 and C16 devices. These values were determined by Simmons fitting using 156 working devices.

increasing molecular length, respectively. The dependence of effective electron mass ($m^* = \alpha^2 m$, where m = electron rest mass) on the molecular length has been studied previously [18, 33]. However, probably due to a lack of analytical data on statistically meaningful devices, the trend for length dependence for Φ_B and α values has not been explained well. In our study, figures 3(a) and (b) show the distributions of Φ_B and α values from the statistically acceptable 156 working devices and clearly show molecular length dependences. The dependence of Φ_B and α values on the tunnelling barrier has been extensively studied for SiO₂ materials. Ng *et al* reported that the Φ_B and effective electron mass values decreased

Table 2. Summary of the statistical average transport parameters of alkanethiol SAMs from all of the working devices. (Note: these parameters were obtained by taking statistical averages from individual parameters of all of the working devices (see text).)

Alkanethiol	J at 1 V			
	(A cm^{-2})	Φ_B (eV)	α	β (\AA^{-1})
C8	$\sim 7.4 \times 10^{-4}$	1.14 ± 0.28	0.76 ± 0.08	0.81 ± 0.05
C12	$\sim 1.4 \times 10^{-3}$	1.26 ± 0.08	0.72 ± 0.04	0.83 ± 0.04
C16	~ 3.4	2.66 ± 0.28	0.52 ± 0.05	0.86 ± 0.06

and increased with decreasing oxide thickness, respectively, which is the same dependence trend found for our alkanethiol molecular systems [29]. The decrease in barrier height was predicted for smaller oxide thickness due to the abrupt nature of the SiO_2/Si interface [30]. The enhancement in effective electron mass with decreasing oxide thickness is presumably due to the modification of the configuration of the Si–O–Si bond in the compressively strained oxide layer near the SiO_2/Si interface [29, 31], or several combined effects of the graded potential drop across the SiO_2/Si interface, the presence of defect-assisted tunnelling and an image force effect [32]. Although our molecular system is not the same as the inorganic SiO_2 layer, the decrease in Φ_B and increase in α (or effective electron mass) with decreasing molecular length may be attributed to a combination of effects such as the different molecular configuration, potential drops at the metal–molecule interface and defect-assisted transport through the molecular layers. Also, note that the Φ_B and α values in figure 3 should be carefully used because the more statistical analysis will give the more accurate parameters.

Although a slight increase in β values with molecular length can be seen (figure 3(c)), the individual β values C8, C12 and C16 devices distributed in the range of 0.7–1.0 \AA^{-1} , which are in agreement with previously reported β values [27, 28, 34]. It should be noted that the α values were less than unity in our experimental results. A lower α value indicates that the potential barrier shape is not rectangular and that tunnelling through alkanethiols may be different from tunnelling through a vacuum. Therefore, the molecular length dependence for α values indicates that the potential barrier shape is also molecular-length-dependent. Englekis *et al* also reported that the Simmons model is inadequate for molecular systems, because of the simplistic model that approximates a single rectangular energy barrier with height Φ_B between two metal electrodes [19]. Hence, the interpretation of potential barrier height Φ_B may be thought of as an effective barrier to charge transport, which may not be the same as the difference in Fermi energy and molecular orbital energy (HOMO, highly occupied molecular orbital in this case) [19].

Table 2 summarizes the electrical transport parameters for Φ_B , α , β values, and the current densities at 1 V for the C8, C12 and C16 alkanethiols, statistically averaged over all the working devices. The average transport parameters do not change significantly with the different criterion ranges (3σ , 2σ or 1σ ranges) for determining acceptable working devices.

When showing device data and doing further analysis such as length-dependent analysis, as in figure 5(a), the task would be tremendous if one were to use all the working devices, 156 devices in our case. Thus, it is

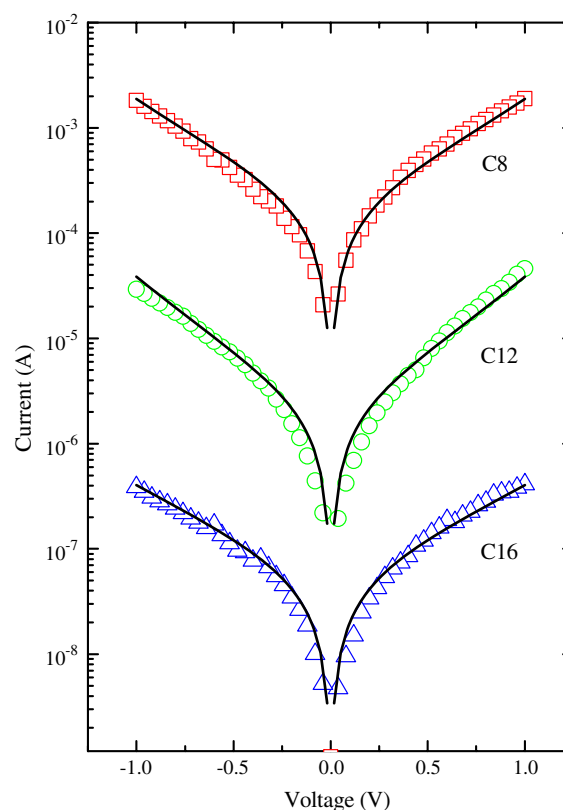


Figure 4. I – V characteristics of three representative devices for three different length alkanethiols (see text regarding the method used to select these representative devices). Symbols are experimental data and solid lines are curves fitted with the Simmons equation.

necessary to choose a few devices that represent the different molecules. Such representative devices can be chosen from the positions of the mean values in the histograms in figure 2 that were used as the criterion for determining working devices. Figure 4 summarizes the I – V characteristics for three representative C8, C12 and C16 devices chosen in this manner, which shows the length-dependent transport properties. Using these representative devices, one can plot a length-dependent tunnelling analysis, a semilog plot of tunnelling current densities at various voltages as a function of the molecular length of the different alkanethiols, as shown in figure 5(a). The tunnelling current densities show an exponential dependence [$J \propto \exp(-\beta d)$] for molecular length. The decay coefficient β values can be determined from the slopes of the line fittings at different biases in figure 5(a) and are plotted in figure 5(b) as a function of bias. The β values obtained here are in the range of 0.83–0.87 \AA^{-1} and are in good agreement with previously reported values for alkanethiols [11]. Both bias dependence [18] and bias independence [27, 34] of β values have been reported. However, we did not observe a bias dependence of decay coefficients as shown in figure 5(b), which may indicate that the barrier lowering effect with applied bias is relatively weak for microscale junction devices, compared with nanometre scale junction devices [18].

The use of the criterion for working devices can be helpful in a research field in which poor device yield is an issue.

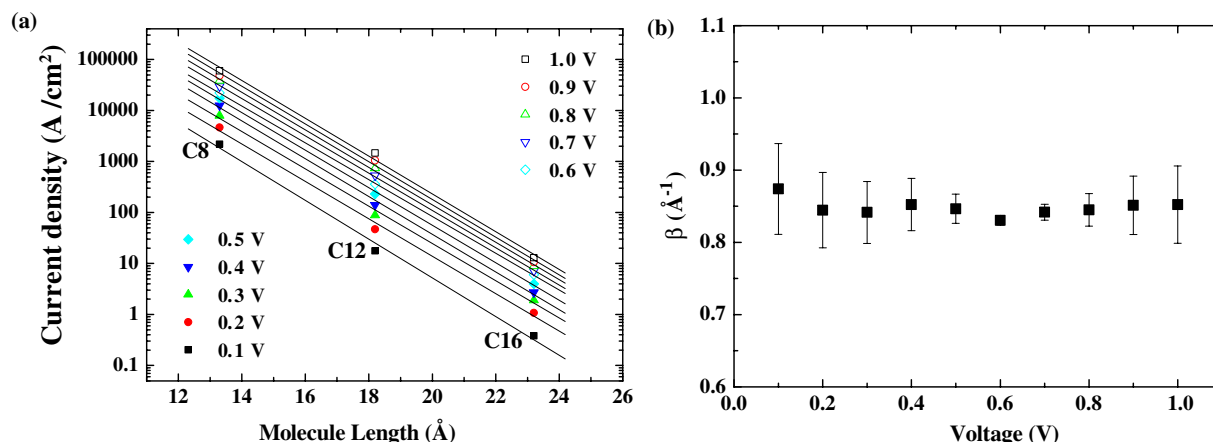


Figure 5. (a) A semilog plot of tunnelling current densities at different biases for three representative alkanethiol devices versus molecular length. The lines through the data points are exponential fittings. (b) Decay coefficient β values obtained from the slope of the exponential fittings as a function of the applied bias.

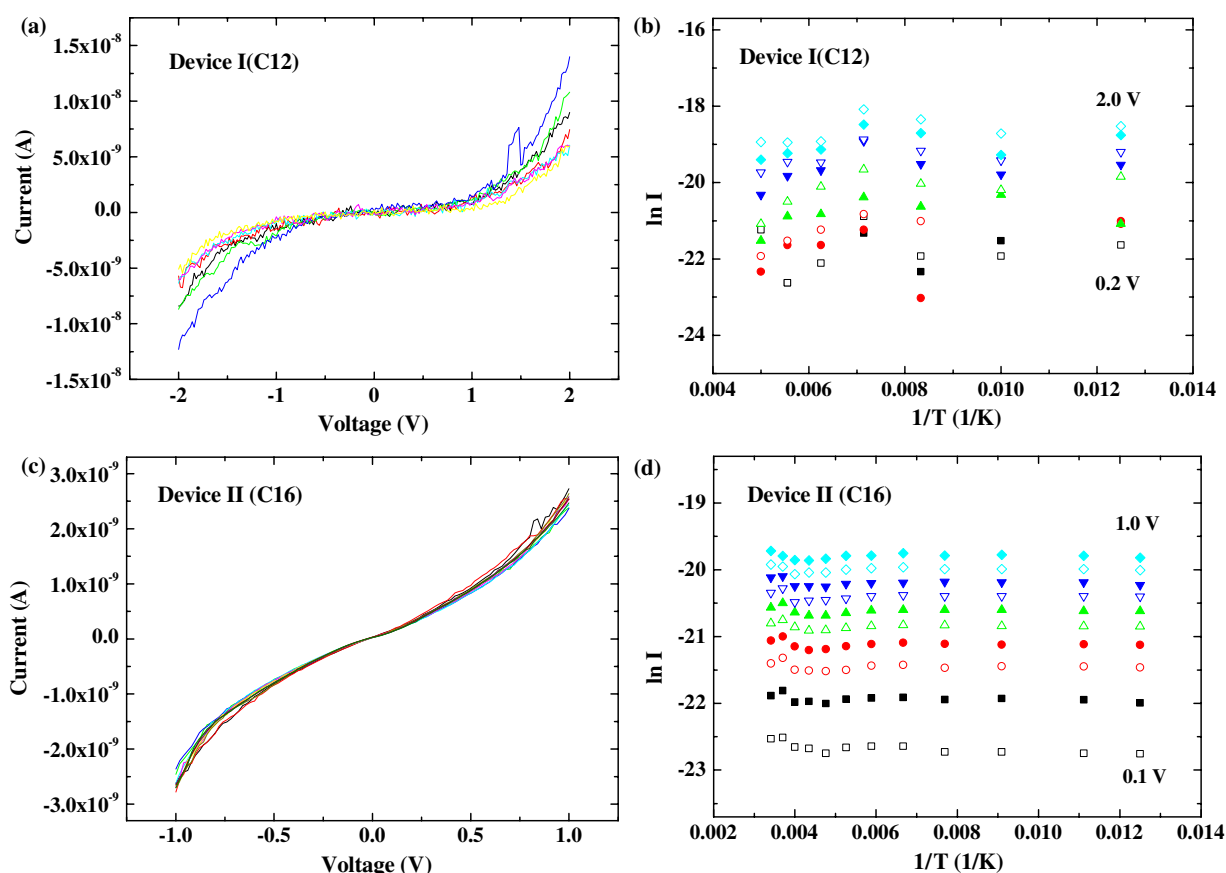


Figure 6. Examples of the temperature-variable I - V characterizations for two devices: Device I (C12) ((a), (b)) and Device II (C16) ((c), (d)). (a) I - V data at temperature from 200 to 80 K with a step of 20 K. (b) Arrhenius plot generated from the I - V data in (a) at voltages from 0.2 to 2.0 V with 0.2 V step. (c) I - V data at temperatures from 280 to 80 K with a step of 20 K. (d) Arrhenius plot generated from the I - V data in (c) at voltages from 0.1 to 1.0 V with 0.1 V step.

For example, to prove the tunnelling transport mechanism, temperature-independent I - V characteristics should be proved from temperature-variable measurements [18]. Figure 6 shows examples of the temperature-variable I - V characteristics (I - V - T) measured from two devices. Although there are slight fluctuations in the I - V - T results (figures 6(a) and (c)), both

devices denoted as Device I (C12) and Device II (C16) show nearly identical tunnelling behaviours, as also explained by temperature independence in an Arrhenius plot analysis (figures 6(b) and (d)). However, Device I is not a working device because the current level is outside the 3σ range (the working device range) for C12 devices, from the histogram in

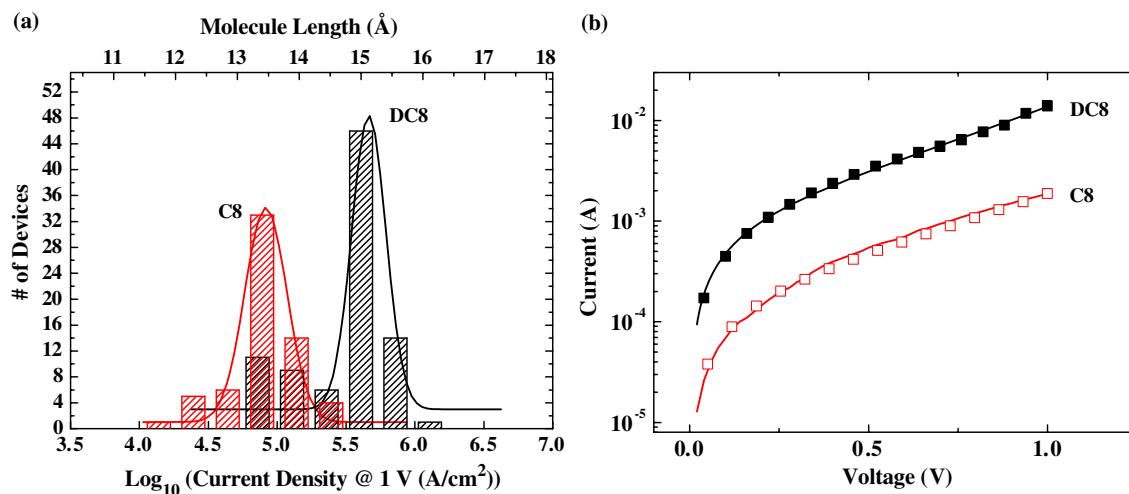


Figure 7. (a) Histogram of logarithmic current densities at 1 V for C8 and DC8 working devices. (b) I - V characteristics of C8 and DC8 representative devices. Symbols are experimental data and solid lines are fitting curves with the Simmons equation.

figure 2(b). In contrast, Device II is within the 3σ range of the histogram for C16 devices (figure 2(b)), and thus it is a working device based on our statistical criterion. This suggests that one should decide whether devices are working or not, before doing any further analysis such as temperature-variable I - V characterizations [18] or inelastic electron tunnelling spectroscopy measurements [35, 36].

The statistical approach to molecular electronic devices can also provide a useful way to distinguish the transport property of different molecular systems. As an example, we performed the statistical analysis on octanedithiol (DC8) devices and compared the charge transport property of DC8 devices with that of octanethiol (C8) devices. As mentioned above, DC8 has thiols [-SH] at both ends and can have chemisorbed contacts [As-S] on both sides of the metal electrodes whereas C8 has a thiol at only one end and thus has only one chemisorbed contact and the other a physisorbed contact [Au-CH₃]. Figure 7(a) shows a histogram of the logarithmic current densities at 1 V for C8 working (63 devices) and DC8 (84 devices) molecular devices after considering the criterion of the working devices to be the 3σ range. The statistical mean current densities of the C8 and DC8 devices were found to be $\sim 74\,000$ and $\sim 355\,000$ A cm⁻² at 1 V, respectively. The current density of DC8 is larger than that of C8 by a factor ~ 5 . Figure 7(b) shows the I - V data for the C8 and DC8 representative devices, chosen from the positions of the mean values in the histogram of figure 7(a). As shown in figure 7(a), the histogram of C8 and DC8 has some overlap range in current densities. In this range, one may make a mistake in data selection of C8 and DC8. Therefore, statistical analysis is necessary to determine the intrinsic property of molecular electronic devices. In this point of view, these results may be a good guide for studying the electronic properties of alkanethiol molecules.

4. Conclusion

We performed a statistical analysis on the electronic transport properties of 13 440 individual molecular electronic devices

in microscale via-hole structures with different lengths of alkanethiols. By using a statistical criterion for defining working devices, we found 156 working alkanethiol devices to be acceptable, while most of the devices were electrical short. Representative devices were chosen from statistical mean positions from the working devices and can be used for further analysis such as a length-dependent tunnelling analysis. The introduction of the statistical consideration of determining the working molecular devices and representative devices can be a meaningful concept to understand electronic transport properties for expanding over organic conducting molecular devices or other devices of nanoscale elements which have typically low device yields and poor reproducibility.

Acknowledgments

We thank A J Heeger, M A Reed and D-Y Kim for helpful discussions and suggestions. This work was supported by grant no. R01-2005-000-10815-0 from the Basic Research Program of the Korea Science and Engineering Foundation and the Program for Integrated Molecular System at GIST. HL acknowledges support from the Creative Research Initiatives (Smart Molecular Memory) of MOST/KOSEF.

References

- [1] Reed M A and Lee T 2003 *Molecular Electronics* (Stevenson Ranch: American Scientific Publishers)
- [2] Nitzan A and Ratner M A 2003 *Science* **300** 1384
- [3] Ulman A 1991 *An Introduction to Ultrathin Organic Films from Langmuir-Blodgett to Self-Assembly* (Boston, CA: Academic)
- [4] Cuniberti G, Fagas G and Richter K 2005 *Introducing Molecular Electronics* (Berlin: Springer)
- [5] Green J E *et al* 2007 *Nature* **445** 414
- [6] Lörtscher E, Cizek J W, Tour J and Riel H 2006 *Small* **2** 973
- [7] Akkerman H B, Blom P W M, de Leeuw D M and de Boer B 2006 *Nature* **441** 69
- [8] Beebe J M, Kim B, Gadzuk J W, Frisbie C D and Kushmerick J G 2006 *Phys. Rev. Lett.* **97** 026801
- [9] Jiang J, Lu W and Luo Y 2004 *Chem. Phys. Lett.* **400** 336

- [10] Lee J O, Lientschnig G, Wiertz F, Struijk M, Janssen R A J, Egberink R, Reinhoudt D N, Hadley P and Dekker C 2003 *Nano Lett.* **3** 113
- [11] Lee T, Wang W, Klemic J F, Zhang J J, Su J and Reed M A 2004 *J. Phys. Chem. B* **108** 8742 and references therein
- [12] González M T, Wu S, Huber R, van der Molen S J, Schönenberger C and Calame M 2006 *Nano Lett.* **6** 2238
- [13] Haick H, Ghabboun J and Cahen D 2005 *Appl. Phys. Lett.* **86** 042113
- [14] Kim T-W, Wang G, Song H, Choi N-J, Lee H and Lee T 2006 *J. Nanosci. Nanotechnol.* **6** 3487
- [15] Song H, Lee H and Lee T 2007 *J. Am. Chem. Soc.* **129** 3806
- [16] Slowinski K, Chamberlain R V, Bilewicz R and Majda M 1996 *J. Am. Chem. Soc.* **118** 4709
- [17] Natelson D 2006 personal communication
- [18] Wang T, Lee T and Reed M A 2003 *Phys. Rev. B* **68** 035416
- [19] Engelkes V B, Beebe J M and Frisbie C D 2004 *J. Am. Chem. Soc.* **126** 14287
- [20] Majumdar N, Gergel N, Routenberg D, Bean J C, Harriott L R, Li B, Pu L, Yao Y and Tour J M 2005 *J. Vac. Sci. Technol. B* **23** 4
- [21] Li X, He J, Hihath J, Xu B, Lindsay S M and Tao N 2006 *J. Am. Chem. Soc.* **128** 2135
- [22] Wang W, Lee T, Kretzschmar I and Reed M A 2004 *Nano Lett.* **4** 643
- [23] Reed M A, Zhou C, Muller C J, Burgin T P and Tour J M 1997 *Science* **278** 252
- [24] Park J *et al* 2002 *Nature* **417** 722
- [25] Simmons J G 1963 *J. Appl. Phys.* **34** 1793
- [26] Wold D J and Frisbie C D 2001 *J. Am. Chem. Soc.* **123** 5549
- [27] Cui X D, Zarate X, Tomfohr J, Sankey O F, Primak A, Moore A L, Moore T A, Gust D, Harris G and Lindsay S M 2002 *Nanotechnology* **13** 5
- [28] Wold D J, Haag R, Rampi M A and Frisbie C D 2002 *J. Phys. Chem. B* **106** 2813
- [29] Ng C Y, Chen T P and Ang C H 2006 *Smart Mater. Struct.* **15** S39
- [30] Lewicki G and Maserjian J 1975 *J. Appl. Phys.* **46** 3032
- [31] Khairurrijal, Mizubayashi W, Miyazaki S and Hirose M 2000 *Appl. Phys. Lett.* **77** 3580
- [32] Städele M, Sacconi F, Di Carlo A and Lugli P 2003 *J. Appl. Phys.* **93** 2681
- [33] Majumdar N, Gergel N, Routenberg D, Bean J C, Harriott L R, Li B, Pu L, Yao Y and Tour J M 2005 *J. Vac. Sci. Technol. B* **23** 1417
- [34] Holmlin R, Haag R, Chabynyc M L, Ismagilov R F, Cohen A E, Terfort A, Rampi M A and Whitesides G M 2001 *J. Am. Chem. Soc.* **123** 5075
- [35] Wang W, Lee T, Kretzschmar I and Reed M A 2004 *Nano Lett.* **4** 643
- [36] Solomon G C, Gagliardi A, Pecchia A, Frauenheim T, Di Carlo A, Reimers J R and Hush N S 2006 *J. Chem. Phys.* **124** 094704